

Tennessee State University

## Digital Scholarship @ Tennessee State University

---

Information Systems and Engineering  
Management Research Publications

Center of Excellence in Information Systems  
and Engineering Management

---

11-1-2006

### HD 71636, A Newly Discovered Eclipsing Binary

Gregory W. Henry

*Tennessee State University*

Francis C. Fekel

*Tennessee State University*

James R. Sowell

*Georgia Institute of Technology*

Joel S. Gearhart

*Georgia Institute of Technology*

Follow this and additional works at: <https://digitalscholarship.tnstate.edu/coe-research>



Part of the [Stars, Interstellar Medium and the Galaxy Commons](#)

---

#### Recommended Citation

Gregory W. Henry et al 2006 AJ 132 2489

This Article is brought to you for free and open access by the Center of Excellence in Information Systems and Engineering Management at Digital Scholarship @ Tennessee State University. It has been accepted for inclusion in Information Systems and Engineering Management Research Publications by an authorized administrator of Digital Scholarship @ Tennessee State University. For more information, please contact [XGE@Tnstate.edu](mailto:XGE@Tnstate.edu).

## HD 71636, A NEWLY DISCOVERED ECLIPSING BINARY

GREGORY W. HENRY AND FRANCIS C. FEKEL<sup>1</sup>

Center of Excellence in Information Systems, Tennessee State University, 3500 John A. Merritt Boulevard, Box 9501, Nashville, TN 37209;  
henry@schwab.tsuniv.edu, fekel@evans.tsuniv.edu

AND

JAMES R. SOWELL AND JOEL S. GEARHART

School of Physics, Georgia Institute of Technology, Atlanta, GA 30332; jim.sowell@physics.gatech.edu

Received 2006 June 21; accepted 2006 August 16

### ABSTRACT

Our differential  $BV$  photometric observations, acquired with an automated telescope at Fairborn Observatory, show that HD 71636 is an eclipsing binary. From follow-up red-wavelength spectroscopic observations we classify the primary and secondary as an F2 dwarf and an F5 dwarf, respectively. The system has a period of 5.01329 days and a circular orbit. We used the Wilson-Devinney program to simultaneously solve our  $BV$  light curves and radial velocities and determined a number of fundamental properties of the system. Comparison with evolutionary tracks indicates that both stars are well ensconced on the main sequence. The age of the system is about 1.2 billion years.

*Key words:* binaries: close — binaries: eclipsing — binaries: spectroscopic

*Online material:* machine-readable table

### 1. INTRODUCTION

HD 71636 = HIP 41691 ( $\alpha = 08^{\text{h}}29^{\text{m}}56^{\text{s}}.31$ ,  $\delta = 37^{\circ}04'15''.5$  [J2000.0]) is a previously unnoteworthy seventh magnitude F star in the constellation of Lynx. Most of what is known about this star comes from various surveys. Olsen (1983) included it in a Strömberg *ubvy* survey of nearly 15,000 stars. From a single observation he determined  $V = 7.88$ . Nordström et al. (2004) observed HD 71636 as part of their very extensive survey of F and G stars in the solar neighborhood. Two CORAVEL measurements resulted in a mean velocity of  $82.7 \text{ km s}^{-1}$ . From the difference between the two velocities Nordström et al. (2004) concluded that HD 71636 is a binary. Its *Hipparcos* parallax is  $0''.00854 \pm 0''.00094$  (Perryman et al. 1997), corresponding to a distance of  $117 \pm 13 \text{ pc}$ . In the Henry Draper Catalogue the star is given a spectral class of F5.

In the *Hipparcos* and Tycho Catalogues (Perryman et al. 1997) the entry for the *Hipparcos* variability type is a blank, indicating that HD 71636 could not be classified as variable or constant because of outliers in the photometry. Henry et al. (2005), however, discovered the star to be an eclipsing binary with a period of approximately 5.013 days after they chose it as the comparison star for differential photometric observations of the  $\gamma$  Doradus variable HD 69715. They continued to use it as their comparison star and simply eliminated their observations of HD 69715 whenever HD 71636 was in eclipse. The *Hipparcos* and Tycho Catalogues failed to recognize HD 71636 as a variable star because all 100 of the *Hipparcos* observations, except for the last two, fell outside the primary and secondary eclipse windows. The last two *Hipparcos* observations were taken consecutively on the same day and fell within secondary eclipse about 0.2 mag below the mean of the other observations.

In this paper we analyze our eclipse observations of HD 71636, which were not included in the Henry et al. (2005) paper, as well as our new spectroscopic observations and determine basic parameters of this binary system.

### 2. PHOTOMETRIC OBSERVATIONS AND REDUCTIONS

As noted in § 1, the photometric observations of HD 71636 in this paper are the same observations that we acquired for Henry et al. (2005) with the T3 0.4 m automatic photoelectric telescope (APT) at Fairborn Observatory. In this paper, however, we included the observations of HD 71636 when it was in eclipse, rather than discarding them as we did in Henry et al. (2005) when we used HD 71636 as a comparison star. Thus, we have a total of 462  $B$  and 456  $V$  observations, all obtained with the T3 0.4 m APT between 2002 September and 2003 May.

The T3 APT uses a temperature-stabilized EMI 9924B photomultiplier tube to acquire data successively through Johnson  $B$  and  $V$  filters. The observations from Henry et al. (2005) and the additional eclipse observations included here were all taken in the following sequence, termed a “group observation”:  $K, S, C, V, C, V, C, V, C, S, K$ , in which  $K$  is the check star (HD 72184;  $V = 5.88$ ,  $B - V = 1.11$ , K2 III),  $C$  is the comparison star (in this case our program star, HD 71636;  $V = 7.88$ ,  $B - V = 0.44$ , F5),  $V$  is the program star (in this case the  $\gamma$  Doradus variable HD 69715;  $V = 7.18$ ,  $B - V = 0.36$ , A5), and  $S$  is a sky reading. Normally three  $V - C$  and two  $K - C$  differential magnitudes are formed from each sequence and averaged together to create group means, which are treated as single observations thereafter. Group mean differential magnitudes with internal standard deviations greater than 0.01 mag are rejected to eliminate observations taken under nonphotometric conditions.

Along with our group measurements of HD 71636, nightly extinction and transformation coefficients were determined from least-squares fits to nightly observations of several dozen standard stars covering a large range of air mass and color index. The  $B$  and  $V$  group mean differential magnitudes that survived the

<sup>1</sup> Visiting Astronomer, Kitt Peak National Observatory, National Optical Astronomy Observatory, operated by the Association of Universities for Research in Astronomy, Inc., under cooperative agreement with the National Science Foundation.

TABLE 1  
PHOTOMETRIC OBSERVATIONS

Heliocentric Julian Date (HJD - 2,400,000)	Phase	$\Delta B$	$\Delta V$
52,539.9899.....	0.5280	+1.993	+1.299
52,540.9877.....	0.7271	+1.998	99.999
52,542.9829.....	0.1251	+1.993	+1.308
52,543.9817.....	0.3243	99.999	+1.298
52,545.9770.....	0.7223	+1.992	+1.293

NOTES.—Table 1 is published in its entirety in the electronic edition of the *Astronomical Journal*. A portion is shown here for guidance regarding its form and content.

0.01 mag cloud filter were corrected for differential extinction and transformed to the Johnson *UBV* system with the following equations (in the notation of Hardie 1962):

$$\Delta B = \Delta_b - k'_b \Delta X + \epsilon_b \Delta(B - V) \quad (1)$$

and

$$\Delta V = \Delta_v - k'_v \Delta X + \epsilon_v \Delta(B - V), \quad (2)$$

where  $k'_b$  and  $k'_v$  are the first-order extinction coefficients and  $\epsilon_v$  and  $\epsilon_b$  are the transformation coefficients. The corrections were applied with nightly extinction coefficients (whose mean values for the year were  $k'_b = 0.282$  and  $k'_v = 0.152$ ) and the yearly mean transformation coefficients  $\epsilon_b = -0.073$  and  $\epsilon_v = -0.079$ . Second-order extinction coefficients were assumed to be  $-0.03$  and  $0.00$  in  $B$  and  $V$ , respectively. Heliocentric corrections were also applied to the times of observation. Further information on the operation of the T3 APT and the analysis of the data can be found in Henry (1995a, 1995b) and Eaton et al. (2003).

Because HD 71636 served as the comparison star in the observing sequence of Henry et al. (2005) and the program star HD 69715 is variable, we created  $C - K$  differential magnitudes to examine the variability in HD 71636. The standard deviation of the  $C - K$  observations, excluding the measures when HD 71636 was in eclipse, is 0.0044 mag (Henry et al. 2005). Therefore, the check star (HD 72184) is constant to the limit of precision of the APT and serves as a satisfactory comparison star for HD 71636. The 462  $B$  and 456  $V C - K$  differential magnitudes are given in Table 1, along with the Heliocentric Julian Dates and orbital phases computed with the photometric ephemeris in § 6.

### 3. SPECTROSCOPIC OBSERVATIONS AND REDUCTIONS

A preliminary photometric eclipse period and epoch produced an ephemeris that was used to determine when to obtain spectra with resolved double lines. From 2003 June to 2004 September, 14 observations were acquired with the coudé feed telescope, coudé spectrograph, and a TI CCD detector at the Kitt Peak National Observatory (KPNO). All the spectrograms are centered at 6430 Å, cover a wavelength range of about 80 Å, and have a resolution of 0.21 Å. The signal-to-noise ratio is typically about 150. Figure 1 presents a spectrum with some lines of the two components identified.

Radial velocities were determined with the IRAF cross-correlation program *fxcor* (Fitzpatrick 1993). Two International Astronomical Union radial velocity standard stars,  $\beta$  Vir and 10 Tau, having adopted velocities of 4.4 and 29.7 km s<sup>-1</sup> (Scarfe et al. 1990), respectively, were used as cross-correlation reference stars.

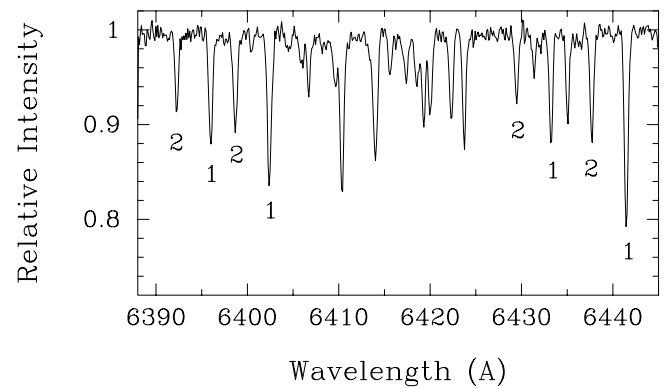


FIG. 1.—Spectrum of HD 71636 in the 6430 Å region. Some lines of the primary, component 1, and secondary, component 2, are identified.

Table 2 lists the radial velocities of both the primary and secondary components, along with the Heliocentric Julian Dates of midobservation.

### 4. SPECTROSCOPIC ORBIT

With an adopted preliminary eclipse period of 5.013 days, an orbital solution of the primary, component 1, was determined with BISP (Wolfe et al. 1967), a computer program that implements a slightly modified version of the Wilsing-Russell method. The orbit was then refined with SB1 (Barker et al. 1967), a program that uses differential corrections. In the same manner an orbit was determined for the secondary, component 2. The variances of the solutions for the primary and secondary were similar, and so all velocities were given unit weights. Then the spectroscopic orbits of the primary and secondary were recomputed with a modified version of SB1, which uses differential corrections to determine simultaneously the elements of the two components. The eccentricity of this solution was extremely small,  $0.0015 \pm 0.0016$ . Thus, a circular-orbit solution was computed with SB2C (D. Barlow 1998, private communication), which also uses differential corrections to determine the elements. The tests of Lucy & Sweeney (1971) indicate that the circular-orbit solution is to be preferred, and so the elements of this spectroscopic solution are given in Table 3. For a circular orbit the element  $T$ , a time of periastron passage, is undefined, and so, as recommended by Batten et al. (1989),  $T_0$ , a time of maximum velocity for the primary, is given instead. Table 2 lists the fractional phases referenced to that epoch and the velocity residuals determined from the circular orbit fit.

### 5. COMBINED LIGHT AND VELOCITY SOLUTION

With the spectroscopic results in hand, combined light and velocity solutions were computed from our observations with the newest version of the Wilson-Devinney (WD) program, which includes the improved stellar atmosphere treatment developed by Van Hamme & Wilson (2003). The program's physical model is described in detail in Wilson & Devinney (1971) and Wilson (1979, 1990). The fitting algorithm is the method of differential corrections, enhanced by a Levenberg-Marquardt procedure to improve convergence (Levenberg 1944; Marquardt 1963). The WD program uses bandpass-integrated fluxes and intensities, which improve light-curve fitting (Williamson et al. 2004). We made simultaneous  $\Delta B$  and  $\Delta V$  light and double-lined radial velocity solutions to improve parameter consistency, as described by Wilson (1979) and Van Hamme & Wilson (1984, 1985). Curve-dependent weights were based on the standard deviations for the whole curves listed in Table 4; the light-level-dependent

TABLE 2  
RADIAL VELOCITIES

Heliocentric Julian Date (HJD - 2,400,000)	Phase	$V_1$ (km s <sup>-1</sup> )	$(O - C)_1$ (km s <sup>-1</sup> )	$V_2$ (km s <sup>-1</sup> )	$(O - C)_2$ (km s <sup>-1</sup> )
52,705.732.....	0.839	+44.5	-0.6	-48.0	-0.6
52,706.788.....	0.049	+79.3	+0.2	-88.0	-0.6
52,708.751.....	0.441	-72.6	-0.3	+90.5	-0.1
52,755.673.....	0.800	+27.8	+0.2	-27.0	-0.1
52,756.655.....	0.996	+83.3	+0.4	-91.6	+0.3
52,757.674.....	0.200	+28.7	+1.1	-26.9	+0.0
52,758.682.....	0.401	-62.0	+0.6	+78.9	-0.3
52,759.707.....	0.605	-60.5	+0.4	+77.8	+0.6
52,760.652.....	0.794	+24.9	+0.6	-23.5	-0.5
52,904.011.....	0.389	-58.7	+0.4	+74.8	-0.3
52,905.001.....	0.587	-66.4	-0.3	+82.5	-0.8
52,941.979.....	0.963	+80.1	-0.6	-89.4	-0.1
53,277.004.....	0.790	+22.7	+0.0	-20.6	+0.5
53,278.010.....	0.991	+82.7	-0.1	-91.5	+0.3

weights were applied in inverse proportion to the square root of the light level.

Our final best-fit light and velocity solution is given in Table 5. The temperature of the hotter component was initially set at 7000 K (Allen 2000), in accordance with the F2 dwarf spectral type determined in § 7. A square root limb-darkening law with coefficients  $x, y$  from Van Hamme (1993) was adopted, and the detailed reflection treatment of Wilson (1990) was used with double reflection. Gravity-darkening ( $g$ ) and bolometric albedo ( $A$ ) coefficients were fixed at canonical values for stars with radiative outer layers (Lucy 1967). After a good intermediate solution was determined, a 50 K grid search was performed to improve the initial temperature assigned to the hotter component. The best-fit solution occurred with  $T_1 = 6950$  K. The internal uncertainty in  $T_1$  was estimated as two 50 K steps, or 100 K. When combined in quadrature with the estimated 100 K temperature scale uncertainty, we estimate the external uncertainty in  $T_1$  to be approximately 140 K. The estimated uncertainty of  $T_2$  was derived from the 10 K error of the temperature difference from the final WD solution added in quadrature to the 140 K estimated external error of  $T_1$ . We also attempted solutions with small (0.5%–5%) amounts of third light, but the WD software always preferred zero values for both the  $B$  and  $V$  passbands with the errors given in Table 5. All remaining uncertainties for the combined light- and velocity-curve parameters in Table 5 are standard deviations

taken directly from the final WD solution. Adopted parameter values are labeled as such. The final goodness-of-fit values (rms) for the two radial velocity and two light curves are given at the bottom of Table 5. We note that these rms values are in very close agreement with the expected precision of the radial velocity and photometric observations.

The WD program provides geometric information about the two components. Relative radii are given in four directions: from the center toward the poles, toward the sides, toward the back (i.e., away from the companion), and toward the inner Lagrangian point, L1. In addition, the program computes “equal volume” mean radii ( $\langle r \rangle$ ) and the percentage of the Roche lobe ( $\langle r \rangle / \langle r \rangle_{\text{lobe}}$ ) that is filled. These parameter values are listed in Table 6, along with their standard deviations from the final WD solution. It is seen that for both components the four directional radii are essentially the same, so the stars are spherically shaped. The Roche lobes are 23% and 21% filled, respectively. Consequently, even though HD 71636 is a rather close binary, it is a well-detached system.

Absolute dimensions of the binary components, based on our final solution listed in Table 5, are given in Table 7. Our absolute dimensions compare well with those of Allen (2000) for F2 V and F5 V stars, although the mass, temperature, and magnitude difference with the hotter star suggests that the secondary component has a slightly later F spectral type.

Figures 2 and 3 present the observed and fitted light curves for the  $\Delta V$  and  $\Delta B$  data, respectively. Inspection of residual plots of the differential  $BV$  data with the theoretical curves shows no asymmetries. Figure 4 presents the radial velocity data plotted with the simultaneous light-velocity solution curve. Zero phase

TABLE 3  
SPECTROSCOPIC ORBITAL ELEMENTS

Parameter	Value
$P$ (days).....	$5.013289 \pm 0.000035$
$T_0$ (HJD).....	$2,452,676.461 \pm 0.0018$
$\gamma$ (km s <sup>-1</sup> ).....	$2.573 \pm 0.098$
$K_1$ (km s <sup>-1</sup> ).....	$80.33 \pm 0.18$
$K_2$ (km s <sup>-1</sup> ).....	$94.48 \pm 0.19$
$e$ .....	0.0 (adopted)
$a_1 \sin i$ (10 <sup>6</sup> km).....	$5.538 \pm 0.013$
$a_2 \sin i$ (10 <sup>6</sup> km).....	$6.513 \pm 0.013$
$m_1 \sin^3 i$ ( $M_\odot$ ).....	$1.5032 \pm 0.0069$
$m_2 \sin^3 i$ ( $M_\odot$ ).....	$1.2780 \pm 0.0063$

NOTE.—Solution computed from spectroscopic data alone with the binary orbit program SB2C.

TABLE 4  
STANDARD DEVIATIONS FOR THE INDIVIDUAL RADIAL VELOCITY AND LIGHT CURVES

Curve	$\sigma^a$
RV primary (km s <sup>-1</sup> ).....	0.54
RV secondary (km s <sup>-1</sup> ).....	0.45
Johnson $V$ .....	0.0047
Johnson $B$ .....	0.0043

<sup>a</sup> For the light curves, in units of total light at phase 0.25.

TABLE 5  
LIGHT- AND VELOCITY-CURVE RESULTS

Parameter	Symbol	Value
Period (days).....	$P$	$5.013292 \pm 0.000023$
Epoch of primary eclipse (HJD).....	$T_0$	$2,452,677.71496 \pm 0.00014$
Eccentricity.....	$e$	0.0 (adopted)
Temperature (K).....	$T_1$	$6950 \pm 140^a$
Temperature (K).....	$T_2$	$6440 \pm 140$
Luminosity ratio ( $V$ ).....	$L_1/(L_1 + L_2)$	$0.6476 \pm 0.0050$
Luminosity ratio ( $B$ ).....	$L_1/(L_1 + L_2)$	$0.6707 \pm 0.0051$
Third light <sup>b</sup> ( $V$ ).....	$l_3$	$0.00 \pm 0.015$
Third light <sup>b</sup> ( $B$ ).....	$l_3$	$0.00 \pm 0.015$
Surface potential.....	$\Omega_1$	$11.9174 \pm 0.0608$
Surface potential.....	$\Omega_2$	$11.9157 \pm 0.0679$
Inclination (deg).....	$i$	$85.634 \pm 0.020$
RV semiamplitude (km s <sup>-1</sup> ).....	$K_1$	$80.55 \pm 0.23$
RV semiamplitude (km s <sup>-1</sup> ).....	$K_2$	$94.87 \pm 0.23$
System velocity (km s <sup>-1</sup> ).....	$V_\gamma$	$2.57 \pm 0.12$
Mass ratio.....	$M_2/M_1$	$0.8491 \pm 0.0028$
Semimajor axis ( $R_\odot$ ).....	$a$	$17.375 \pm 0.032$
Limb darkening (bolometric).....	$x_1, y_1$	$+0.090, +0.635$ (adopted)
Limb darkening (bolometric).....	$x_2, y_2$	$+0.121, +0.598$ (adopted)
Limb darkening ( $V$ ).....	$x_1, y_1$	$+0.061, +0.725$ (adopted)
Limb darkening ( $B$ ).....	$x_1, y_1$	$+0.184, +0.697$ (adopted)
Limb darkening ( $V$ ).....	$x_2, y_2$	$+0.112, +0.691$ (adopted)
Limb darkening ( $B$ ).....	$x_2, y_2$	$+0.295, +0.589$ (adopted)
Albedo (bolometric).....	$A_1, A_2$	0.5, 0.5 (adopted)
Gravity darkening.....	$g_1, g_2$	0.3, 0.3 (adopted)
Rotation/orbit ratio.....	$F_1, F_2$	1.0, 1.0 (adopted)
rms (RV <sub>1</sub> ) (km s <sup>-1</sup> ).....	...	0.52
rms (RV <sub>2</sub> ) (km s <sup>-1</sup> ).....	...	0.46
rms ( $V$ ) <sup>c</sup> .....	...	0.0047
rms ( $B$ ) <sup>c</sup> .....	...	0.0043

NOTES.—Limb-darkening coefficients are for a square root law (Van Hamme 1993). The table gives the WD simultaneous solution, including proximity effects, of the light and velocity data.

<sup>a</sup> Based on the estimated F2 V spectral type and improved by a grid search.

<sup>b</sup> In units of total light at phase 0.25.

<sup>c</sup> The rms residuals in units of total light at phase 0.25.

is a time of primary eclipse, and so the phases shown there are 0.25 larger than those listed in Table 2.

## 6. EPHEMERIS PARAMETERS

For the light- and velocity-curve solutions described in § 5, we used time (HJD) instead of phase as the independent variable. This allowed us to determine ephemeris parameters (reference

epoch  $T_0$  and period  $P$ ) as part of the solution. These parameters are now based on whole light and velocity curves, not just on times of minima. Examples of this method, including checks against ephemeris parameters based on eclipse timings, can be found in Van Hamme et al. (2001) for CN And and in Williamon et al. (2005) for AR Mon.

The ephemeris for primary eclipse of HD 71636 is

$$\begin{aligned} \text{Minimum Light (HJD)} &= 2,452,677.71496 \pm 0.00014 \\ &+ 5.013292 \pm 0.000023E. \end{aligned}$$

TABLE 6  
MODEL RADII

Parameter	Value
$r_1$ (pole).....	$0.0903 \pm 0.0005$
$r_1$ (point).....	$0.0905 \pm 0.0005$
$r_1$ (side).....	$0.0904 \pm 0.0005$
$r_1$ (back).....	$0.0905 \pm 0.0005$
$\langle r_1 \rangle^a$ .....	$0.0904 \pm 0.0005$
$\langle r_1 \rangle / \langle r_1 \rangle_{\text{lobe}}$ .....	$0.2292 \pm 0.0013$
$r_2$ (pole).....	$0.0783 \pm 0.0005$
$r_2$ (point).....	$0.0784 \pm 0.0005$
$r_2$ (side).....	$0.0783 \pm 0.0005$
$r_2$ (back).....	$0.0784 \pm 0.0005$
$\langle r_2 \rangle^a$ .....	$0.0784 \pm 0.0005$
$\langle r_2 \rangle / \langle r_2 \rangle_{\text{lobe}}$ .....	$0.2144 \pm 0.0014$

<sup>a</sup> Equal volume mean radii.

TABLE 7  
FUNDAMENTAL PARAMETERS

Parameter	Primary Star	Secondary Star
$V$ (mag).....	8.35	9.01
$B - V$ (mag).....	0.37	0.48
Spectral type.....	F2 dwarf	F5 dwarf
$M$ ( $M_\odot$ ).....	$1.513 \pm 0.009$	$1.285 \pm 0.007$
$R$ ( $R_\odot$ ).....	$1.571 \pm 0.009$	$1.361 \pm 0.008$
$\log(L/L_\odot)$ .....	$0.713 \pm 0.036$	$0.457 \pm 0.038$
$M_{\text{bol}}$ .....	$2.96 \pm 0.09$	$3.60 \pm 0.09$
$\log g$ (cm s <sup>-2</sup> ).....	$4.23 \pm 0.01$	$4.28 \pm 0.01$
$v_{\text{rot}}$ (km s <sup>-1</sup> ).....	$12.5 \pm 1.0$	$12.4 \pm 1.0$

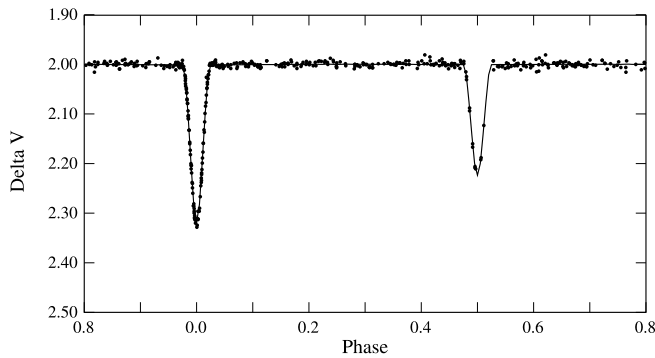


FIG. 2.—Differential  $V$  magnitudes of HD 71636 plotted with the computed solution curve.

The spectroscopic ephemeris, listed in Table 3, of

$$\begin{aligned} \text{maximum velocity (HJD)} &= 2,452,676.461 \pm 0.0018 \\ &+ 5.013289 \pm 0.000035E, \end{aligned}$$

compares very well with the combined solution. The periods are almost identical, and the 1.25396 day difference in  $T_0$  is equal to 0.250 units in phase.

## 7. SPECTRAL TYPES AND MAGNITUDE DIFFERENCE

Strassmeier & Fekel (1990) identified several luminosity-sensitive and temperature-sensitive line ratios in the 6430–6465 Å region. Those critical line ratios and the general appearance of the spectrum were employed as spectral-type criteria. However, for stars earlier than early-G spectral class, the line ratios in the 6430 Å region have little sensitivity to luminosity. The masses of the two stars compared with canonical values from Gray (1992) and Allen (2000), as well as the spectral class of F5 for the HD 71636 system in the Henry Draper Catalogue, indicate that both components are likely F stars. Thus, we can only determine the spectral classes of the two components. However, the absolute visual magnitudes of the components, determined with the *Hipparcos* parallax of  $0''.00854$ , indicate that both stars are dwarfs. Thus, the spectrum of HD 71636 was compared with those of late-A, as well as early- and mid-F, dwarfs from the lists of Abt & Morrell (1995) and Fekel (1997). Spectra of those reference stars were obtained at KPNO with the same telescope, spectrograph, and detector as our spectra of HD 71636. With a computer program developed by Huenemoerder & Barden (1984) and Barden (1985) various combinations of reference-star spectra were rotationally broadened, shifted in radial velocity, appropri-

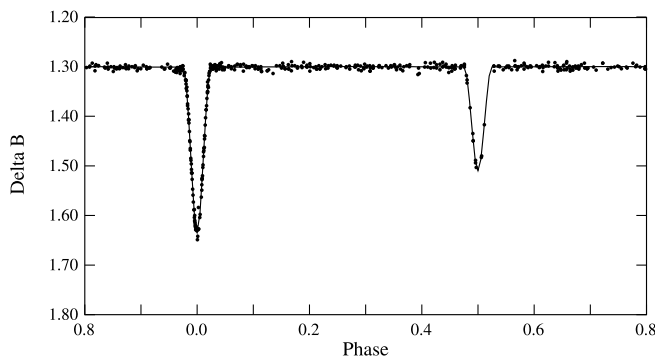


FIG. 3.—Differential  $B$  magnitudes of HD 71636 plotted with the computed solution curve.

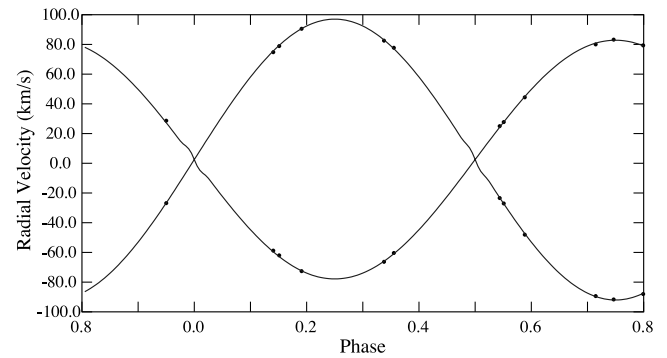


FIG. 4.—HD 71636 radial velocities and computed curves for the simultaneous light and velocity solution including proximity effects.

ately weighted, and added together in an attempt to reproduce the spectrum of HD 71636 in the 6430 Å region. The best fit to its spectrum was found with a combination of HR 5075 (F2 V [Abt & Morrell 1995] and  $[\text{Fe}/\text{H}] = -0.04$  [Boesgaard & Tripicco 1986]) plus HR 2943 (F5 IV–V [Johnson & Morgan 1953] and mean  $[\text{Fe}/\text{H}] = -0.02$  [Taylor 2003]). The iron abundances of the reference stars suggest that HD 71636 has an iron abundance that may be slightly less than the Sun's. This is consistent with a mean  $[\text{Fe}/\text{H}] = -0.09$  for the combined system, determined by Nordström et al. (2004) from Strömgren photometry.

The resulting continuum-intensity ratio is  $I_2/I_1 = 0.553$ . Because of the similarity of the spectral types, we adopt this value as the luminosity ratio, which corresponds to a magnitude difference of 0.64 in the 6430 Å region. This central wavelength is about 0.6 of the way between the effective wavelengths of the Johnson  $V$  and  $R$  bandpasses. Thus, from the mean colors of F2 and F5 dwarfs (Johnson 1966), for HD 71636 we determine  $\Delta V = 0.6$  mag and estimate an uncertainty of 0.1 mag. This result is in agreement with the more precise determination of 0.66 mag from the light-curve solution (see Table 7).

## 8. CIRCULARIZATION AND SYNCHRONIZATION

It is well known (e.g., Tassoul & Tassoul 1996) that tidal interactions affect the rotational and orbital characteristics of close binaries, causing them to tend toward a state in which the rotational axes of the components are parallel to the orbital axis and their rotational velocities are synchronized with the orbital period. In addition, tidal dissipation of energy causes a binary to circularize its orbit. Indeed, observational results indicate that many binaries have fully accomplished these feats. Other systems with weaker tidal interactions may not be currently old enough to have reached complete synchronization or circularization. However, these conditions may occur once tidal interactions have acted long enough or after a system evolves to a state in which tidal interactions are enhanced.

While A stars have radiative outer atmospheres, early-F stars begin to have very thin convective outer atmospheres (Böhm-Vitense 1992, pp. 81–83), and the convection zone of a star increases in depth as the effective surface temperature decreases. Thus, the primary and secondary components of HD 71636, with spectral types of F2 dwarf and F5 dwarf, respectively, have rather thin convective envelopes.

For stars with convective envelopes, Zahn (1977, 1989) investigated the effects of the equilibrium tide on synchronization and circularization, while Tassoul (1987, 1988) explored the theory that binary synchronization and circularization result because of distortions that cause large-scale hydrodynamic currents. Although these two theories disagree significantly on absolute

timescales, both predict that synchronization should occur before circularization.

To examine the possibility of synchronization, we first determined the projected rotational velocities of the two components. We analyzed 10 KPNO red-wavelength spectra with the procedure of Fekel (1997). For each spectrum the full width at half-maximum of two to four moderate-strength or weak lines was measured, and the results were averaged for each component. The instrumental broadening was removed, and the calibration polynomial of Fekel (1997) was used to convert the resulting broadening in angstroms into a total line broadening in kilometers per second. Following Fekel (1997) we adopted a macro-turbulence of  $5 \text{ km s}^{-1}$  for the primary and  $4 \text{ km s}^{-1}$  for the secondary. The resulting  $v \sin i$  values are  $12.5$  and  $12.4 \text{ km s}^{-1}$  for components 1 and 2, respectively, with an estimated error of  $1 \text{ km s}^{-1}$ . We next assumed that the orbital and rotational axes are parallel, so from the solution of the light curve the rotational inclination is  $85.6^\circ$ . Because it is so close to  $90^\circ$ , we adopted our  $v \sin i$  values as the equatorial rotational velocities of the components. From Table 7 the radii are  $1.57$  and  $1.36 R_\odot$  for the primary and secondary, respectively. Those values, combined with the orbital period of  $5.013$  days, lead to rotational velocities of  $15.8$  and  $13.7 \text{ km s}^{-1}$ . Thus, the rotation of the primary is slightly slower than its synchronous value, while the secondary, which has the slightly deeper convective outer atmosphere, may well be rotating synchronously.

As noted in § 4, the computed eccentricity of the spectroscopic orbit is extremely small,  $0.0015 \pm 0.0016$ . Thus, we have adopted a circular orbit, a result supported by our photometric solution.

## 9. DISCUSSION

### 9.1. Reddening?

To determine  $B - V$  colors for the individual components, we first computed  $\Delta B = 0.77$  mag and  $\Delta V = 0.66$  mag from the  $B$  and  $V$  luminosity ratios (Table 5), respectively. Adopting  $V = 7.88$  mag from Olsen (1983) as the combined magnitude of the system produces  $V_1 = 8.35$  and  $V_2 = 9.01$  mag. To determine the combined  $B$  magnitude of the system, we determined a mean out-of-eclipse  $\Delta B = 1.30$  mag between HD 71636 and HD 72184. For HD 72184  $V = 5.88$  mag (Perryman et al. 1997) and  $B - V = 1.11$  mag, producing  $B = 6.99$  mag. Thus, for the HD 71636 system  $B = 8.29$  mag, and its  $B - V = 0.41$  mag. This results in  $B - V = 0.37$  mag for the primary and  $0.48$  mag for the secondary. Using the  $(B - V) - T_{\text{eff}}$  calibration of Flower (1996) we find that our effective temperatures for the binary components from our WD solution result in  $B - V$  colors of  $0.35$  and  $0.46$  mag. This suggests that the system may be slightly reddened by  $0.02$  mag, a result consistent with its distance of  $117 \pm 13$  pc.

### 9.2. Evolutionary Status

Because HD 71636 is a well-detached system and both stars are dwarfs, it is reasonable to assume that there has been no exchange or loss of mass and that the stars' evolutionary states can be estimated from single-star evolutionary models. As indicated in § 7, the components appear to have near-solar abundances. Thus, we have located the primary and secondary in a theoretical H-R diagram (Fig. 5) and compared their positions with solar abundance evolutionary tracks for  $1.2$ ,  $1.3$ , and  $1.5 M_\odot$  stars computed by Girardi et al. (2000). Note that the error bars in Figure 5 are larger than those listed in Table 7. Errors in  $\log(L/L_\odot)$  and  $M_{\text{bol}}$  in Table 7 are computed from errors in temperature and radius. Because in the light and velocity solution the mean surface temperature of the primary component is not an adjusted

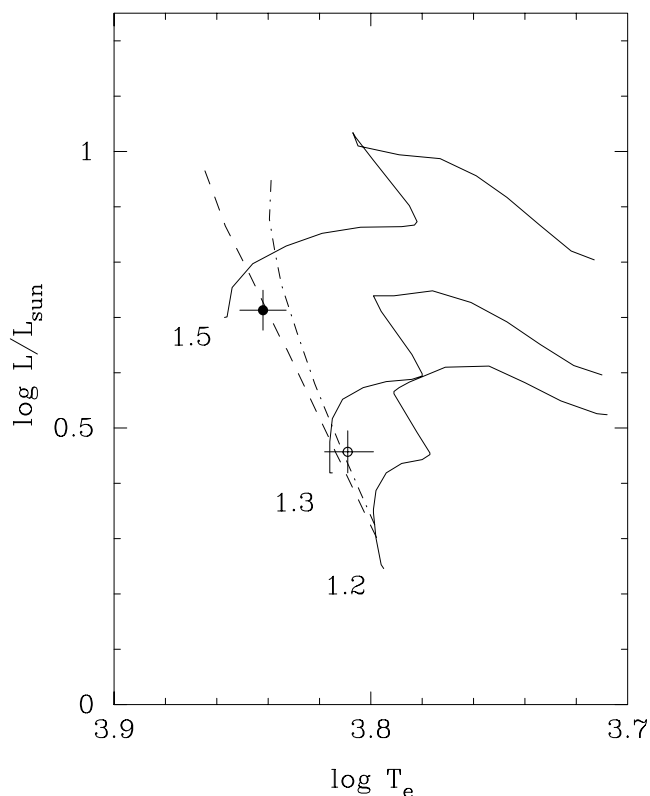


FIG. 5.— Positions of the F2 dwarf primary (filled circle) and the F5 dwarf secondary (open circle) in a theoretical H-R diagram. The positions of the components are compared to the  $1.2$ ,  $1.3$ , and  $1.5 M_\odot$  solar abundance evolutionary tracks of Girardi et al. (2000), as well as their  $1.0$  billion year (dashed line) and  $1.41$  billion year (dash-dotted line) isochrones.

parameter, it has no formal error. However, in § 5 we estimated uncertainties of  $140 \text{ K}$  for the effective temperatures of the primary and secondary and used those errors to compute the uncertainties of the luminosities of the two components. The masses predicted by the evolutionary tracks are  $1.45$  and  $1.27 M_\odot$  for the primary and secondary, respectively, compared with our observationally determined values of  $1.51$  and  $1.28 M_\odot$ . Thus, the theoretical secondary mass is in good agreement with the observation, while the theoretical mass of the primary is  $0.06 M_\odot$  too large. The figure also shows the  $1.0$  and  $1.41$  billion year isochrones (Girardi et al. 2000), from which the age of the system is  $1.2 \pm 0.2$  billion years.

A comparison of the components with the models of Girardi et al. (2000) in a plot of surface gravity versus effective temperature ( $\log g$  vs.  $\log T_e$ ) again produces good agreement for the secondary but not for the primary.

We also compared the positions of our components in an H-R diagram with the latest set of solar abundance evolutionary tracks from the Yonsei-Yale models (Demarque et al. 2004). Their models are computed with physics similar to that of Girardi et al. (2000) but differ in a number of details. The Yonsei-Yale evolutionary tracks are in better agreement with the mass of the primary but are in worse agreement with the mass of the secondary.

### 9.3. Space Motion

Using their mean radial velocity of  $82.7 \text{ km s}^{-1}$  as the systemic radial velocity, Nordström et al. (2004) computed the  $U$ ,  $V$ ,  $W$  space motions of HD 71636 in a right-handed coordinate system. Their large systemic velocity led to large  $U$  and  $W$  velocities. Our systemic velocity of  $2.6 \text{ km s}^{-1}$  (Table 3) differs from their adopted

value by  $80 \text{ km s}^{-1}$ . Thus, we have recomputed the space motions, obtaining  $-1$ ,  $-3$ , and  $2 \text{ km s}^{-1}$  for  $U$ ,  $V$ , and  $W$ , respectively.

We thank Lou Boyd at Fairborn for making our automated photometry possible. This research at Tennessee State Univer-

sity was supported in part by NASA grant NCC5-511 and NSF grant HRD-9706268. This research has made use of the SIMBAD database, operated at CDS, Strasbourg, France. The authors also wish to thank W. Van Hamme for his assistance with aspects and error bars pertaining to the final WD combined light-velocity solutions.

## REFERENCES

- Abt, H. A., & Morrell, N. 1995, *ApJS*, 99, 135  
 Allen, C. W. 2000, in *Allen's Astrophysical Quantities*, ed. A. N. Cox (New York: Springer), 388  
 Barden, S. C. 1985, *ApJ*, 295, 162  
 Barker, E. S., Evans, D. S., & Laing, J. D. 1967, *R. Obs. Bull.*, 130, 355  
 Batten, A. H., Fletcher, J. M., & MacCarthy, D. G. 1989, *Publ. Dominion Astrophys. Obs.*, 17, 1  
 Boesgaard, A. M., & Tripicco, M. J. 1986, *ApJ*, 303, 724  
 Böhm-Vitense, E. 1992, *Introduction to Stellar Astrophysics*, Volume 3 (Cambridge: Cambridge Univ. Press)  
 Demarque, P., Woo, J.-H., Kim, Y.-C., & Yi, S. K. 2004, *ApJS*, 155, 667  
 Eaton, J. A., Henry, G. W., & Fekel, F. C. 2003, in *The Future of Small Telescopes in the New Millennium*, Volume II: The Telescopes We Use, ed. T. D. Oswalt (Dordrecht: Kluwer), 189  
 Fekel, F. C. 1997, *PASP*, 109, 514  
 Fitzpatrick, M. J. 1993, in *ASP Conf. Ser. 52, Astronomical Data Analysis Software and Systems II*, ed. R. J. Hanisch, R. V. J. Brissenden, & J. Barnes (San Francisco: ASP), 472  
 Flower, P. J. 1996, *ApJ*, 469, 355  
 Girardi, L., Bressan, A., Bertelli, G., & Chiosi, C. 2000, *A&AS*, 141, 371  
 Gray, D. F. 1992, *The Observation and Analysis of Stellar Photospheres* (Cambridge: Cambridge Univ. Press)  
 Hardie, R. H. 1962, in *Astronomical Techniques*, Volume 2: Stars and Stellar Systems, ed. W. A. Hiltner (Chicago: Univ. Chicago Press), 178  
 Henry, G. W. 1995a, in *ASP Conf. Ser. 79, Robotic Telescopes: Current Capabilities, Present Developments, and Future Prospects for Automated Astronomy*, ed. G. W. Henry & J. A. Eaton (San Francisco: ASP), 37  
 ———. 1995b, in *ASP Conf. Ser. 79, Robotic Telescopes: Current Capabilities, Present Developments, and Future Prospects for Automated Astronomy*, ed. G. W. Henry & J. A. Eaton (San Francisco: ASP), 44  
 Henry, G. W., Fekel, F. C., & Henry, S. M. 2005, *AJ*, 129, 2815  
 Huenemoerder, D. P., & Barden, S. C. 1984, *BAAS*, 16, 510  
 Johnson, H. L. 1966, *ARA&A*, 4, 193  
 Johnson, H. L., & Morgan, W. W. 1953, *ApJ*, 117, 313  
 Levenberg, K. 1944, *Q. J. Appl. Math.*, 11, 431  
 Lucy, L. B. 1967, *Z. Astrophys.*, 65, 89  
 Lucy, L. B., & Sweeney, M. A. 1971, *AJ*, 76, 544  
 Marquardt, D. W. 1963, *SIAM J. Appl. Math.*, 11, 431  
 Nordström, B., et al. 2004, *A&A*, 418, 989  
 Olsen, E. H. 1983, *A&AS*, 54, 55  
 Perryman, M. A. C., et al. 1997, *The Hipparcos and Tycho Catalogues* (ESA SP-1200; Noordwijk: ESA)  
 Scarfe, C. D., Batten, A. H., & Fletcher, J. M. 1990, *Publ. Dominion Astrophys. Obs.*, 18, 21  
 Strassmeier, K. G., & Fekel, F. C. 1990, *A&A*, 230, 389  
 Tassoul, J.-L. 1987, *ApJ*, 322, 856  
 ———. 1988, *ApJ*, 324, L71  
 Tassoul, J.-L., & Tassoul, M. 1996, *Fundam. Cosm. Phys.*, 16, 337  
 Taylor, B. J. 2003, *A&A*, 398, 731  
 Van Hamme, W. 1993, *AJ*, 106, 2096  
 Van Hamme, W., Samec, R. G., Gothard, N. W., Wilson, R. E., Faulkner, D. R., & Branly, R. M. 2001, *AJ*, 122, 3436  
 Van Hamme, W., & Wilson, R. E. 1984, *A&A*, 141, 1  
 ———. 1985, *Ap&SS*, 110, 169  
 ———. 2003, in *ASP Conf. Ser. 298, GAIA Spectroscopy, Science and Technology*, ed. U. Munari (San Francisco: ASP), 323  
 Williamon, R. M., Sowell, J. R., & Van Hamme, W. 2004, *AJ*, 128, 1319  
 Williamon, R. M., Van Hamme, W., Torres, G., Sowell, J. R., & Ponce, V. C. 2005, *AJ*, 129, 2798  
 Wilson, R. E. 1979, *ApJ*, 234, 1054  
 ———. 1990, *ApJ*, 356, 613  
 Wilson, R. E., & Devinney, E. J. 1971, *ApJ*, 166, 605  
 Wolfe, R. H., Horak, H. G., & Storer, N. W. 1967, in *Modern Astrophysics*, ed. M. Hack (New York: Gordon & Breach), 251  
 Zahn, J.-P. 1977, *A&A*, 57, 383  
 ———. 1989, *A&A*, 220, 112